ELSEVIER

Aquatic Botany 79 (2004) 211–234

Aquatic botany

www.elsevier.com/locate/aquabot

Modeling growth and carbon allocation in two reed beds (*Phragmites australis*) in the Scheldt estuary

Karline Soetaert [a,*], Maurice Hoffmann [b], Patrick Meire [c], Mathieu Starink [a], Dick van Oevelen [a], Sabine Van Regenmortel [c], Tom Cox [c]

[a] *Centre for Estuarine and Marine Ecology, Netherlands Institute of Ecology, PB 140, 4400 AC, Yerseke, The Netherlands*

[b] *Institute of Nature Conservation, Kliniekstraat 25, 1070 Brussels, Belgium*

[c] *Department Biology, University Antwerp, Universiteitsplein 1C, 2610 Wilrijk, Belgium*

Received 15 January 2003; received in revised form 17 December 2003; accepted 3 February 2004

Abstract

Common reed (*Phragmites australis*) is a prominent species in the upstream part of the eutrophic Scheldt estuary (Belgium, The Netherlands). From 1996 till 1998, seasonal growth dynamics of the species were studied in two monospecific stands subjected to different salinity regimes (seasonal means 1.6 and 13.3 PSU, respectively). We addressed the following questions: how are these reed vegetations affected by meteorological conditions and by the growth site, what are the important growth processes and what is the fate of the annually fixed carbon. A mathematical model was developed and calibrated using the data from the oligohaline site. Subsequent application of the model to the mesohaline stand required adaptation of parameters relating to the partitioning of resources and timing of growth initiation only. At their peak, the aboveground biomass was 587–1678 g DW m^{-2} at the 13.3 PSU site and 1116–2179 g DW m^{-2} (1.6 PSU); more than 60% of the biomass was located underground. In 1996, biomasses were 2–3 times lower than in the other 2 years, caused by a retarded growth initiation. Probably due to a lower temperature in early 1996, rhizome bud burst occurred more than 1 month later compared to the other years. In addition, growth initiation was several weeks later in the mesohaline site. This appeared mainly responsible for the large difference in maximal aboveground biomass between both stations. Architecture of the plants was also affected, with a higher shoot density (about 50% more shoots), better-developed root system (15% of total belowground biomass compared to 5%) and more, but smaller leaves at the higher salinity site. Notwithstanding large differences in aboveground biomass, annual growth was similar at both stations (154 and 132 mol C m^{-2} per year at the oligo- and mesohaline station, respectively). Primary production accounted for about 80% of all growth processes, rhizome

* Corresponding author. Tel.: +31-113-577487; fax: +31-113-573616.
E-mail address: k.soetaert@nioo.knaw.nl (K. Soetaert).

doi:10.1016/j.aquabot.2004.02.001

remobilization for almost 20%, translocation of mass before sloughing of leaves accounting about 3%. Within a year, some 44% (oligohaline) and 36% (mesohaline) of new assimilates produced by photosynthesis accumulated as dead litter. The other part was respired by the plant itself, either to provide the energy for growth (23%) or maintenance costs (33–41% at the oligo- and mesohaline station, respectively). Calculated annual turnover rates of aboveground biomass, rhizomes and roots were 100, 62 and 73%, respectively.

Keywords: Carbon budget; Numerical model; Growth model; Interannual variation; Estuary

1. Introduction

Phragmites australis (Trin. Ex Steud.), the perennial grass known as common reed, is one of the most widely distributed plant species on earth. It is common in wetland habitats such as marshes and the littoral zone of lakes, rivers and estuaries where it is found in specific zones with respect to water level (Coops et al., 1996; Vretare et al., 2001), tidal elevation (Squires and Van der Valk, 1992; Chambers, 1997), wave action (Coops et al., 1991), salinity in water and soil (Burdick et al., 2001) and redox conditions of the soil (Weisner, 1996; Van der Putten, 1997; Sanchez et al., 1998).

Although a freshwater species, reed is salt tolerant and often invades brackish or marine areas. Typically it does not thrive above a salinity of 15–20 PSU (e.g. Lissner and Schierup, 1997; Hootsmans and Wiegman, 1998), except where its deep roots can access low-salinity waters (Lissner and Schierup, 1997; Adams and Bate, 1999). There is evidence that salinity affects both the production (Mauchamp and Mesleard, 2001; Hanganu et al., 1999; Zhao et al., 1999) and morphology of reed (Hellings and Gallagher, 1992; Rolletschek and Hartzendorf, 2000).

Healthy reed stands are highly productive (e.g. Windham and Lathrop, 1999). Reported maximal aboveground biomass varies between 152 (Rolletschek et al., 1999) and 7700 DW m^{-2} (Rolletschek and Hartzendorf, 2000), and is typically around 1000 g DW m^{-2}. Statistical analysis has revealed that densities, biomasses and morphological characteristics of reeds depend on latitude (e.g. Clevering, 1999; Ostendorp et al., 2001; Lessmann et al., 2001), climate (Klimes et al., 1999), salinity (Hootsmans and Wiegman, 1998; Adams and Bate, 1999), water depth (Weisner and Strand, 1996), eutrophication (Kühl and Kohl, 1992; Kohl et al., 1998) and interactions between these factors (Lissner et al., 1999). However, these tendencies may be confounded by large yearly fluctuations in biomass (e.g. Boar, 1996).

With little external loss, the maximal aboveground stocks are generally assumed to be within 85–100% of net annual aboveground production (Gessner et al., 1996; Brix et al., 2001). A variable part of this aboveground production ends up as dead litter, which may constitute a considerable portion of the detrital mass in the habitat and enter the diet of animals (Boschker et al., 1995). There is ample documentation in the literature of the maximal aboveground biomass of reed and hence net aboveground production. However, the increase of aboveground reed biomass is a complex function of new production, accomplished by photosynthesis, of regenerated production, through remobilisation of rhizome biomass and

shoots and of dissimilatory processes. The quantification of (some of) these specific processes and the fate of the production have been dealt with only in few studies. Allirand and Gosse (1995) interpreted the accumulation of aboveground matter by means of a so-called agro-meteorological model for a reed stand in France. In this approach, a discontinuity in the relationship between photosynthetically active radiation accumulated by a canopy versus the standing stock of the aboveground organs is taken as indicative for the cessation of rhizome remobilisation. Alternatively, Boar (1996 and references herein) used the changes in rhizome biomass within a year as a measure of the degree of rhizome remobilisation. Other researchers have dealt with the degree of export production, which is measured as the amount of dead material at the onset of senescence (e.g. Gessner, 2001). Coupled mathematical models use a larger variety of data, and therefore, may derive a better-constrained and more complete budget. Asaeda and Karunaratne (2000) and Karunaratne and Asaeda (2000) were the first to apply such a dynamic model for reed growth.

The Scheldt river and upstream part of the estuary is an area where reed stands dominate the interface between land and water (Van Damme et al., 1999; Van der Nat and Middelburg, 2000). This study deals with two reed stands in the Scheldt estuary, differing in their salinity regime. We address the following questions: how are these reed vegetations affected by meteorological and growth site conditions, how does this affect their production and the internal cycling of matter, how much of the annually fixed carbon is retained in rhizome storage and how much is lost as detritus or dissolved organic matter. To do so we have developed a dynamic mathematical model that describes the growth dynamics and cycling of carbon amongst the various organs. We used an extensive dataset, compiled at the two Scheldt sites and that covers both living and dead biomass to calibrate and validate the model.

1.1. Data collection and processing

The data were collected along two sites in the Scheldt estuary (Table 1). This is a 160 km long macrotidal estuary (tidal amplitude 2–5 m) with a mean annual freshwater discharge of 100 $m^3 s^{-1}$. Tidal influence penetrates upstream till North of the city of Ghent (Belgium). The Scheldt river and estuary flows through highly urbanised, agricultural and industrial land in France, Belgium and The Netherlands. High nutrient loadings and sewage have seriously degraded the water quality, mainly in the most upstream part of the estuary where low oxygen concentrations are commonly observed (Soetaert and Herman, 1995).

Healthy, fringing reeds are common mainly in the fresh and oligohaline part of the Scheldt estuary (Van Damme et al., 1999). In the most upstream zone, at mean salinities below 1.5 PSU, *Salix* communities dominate but reed is the most prominent member of the herbaceous

Table 1
Abiotic characteristics of the two stations

Station	Saeftinghe	Burcht
Location	51°20′N 4°14E	51°10′N 4°25E
Salinity (PSU)	13.3 (4.5–20) ($N = 33$)	1.6 (0.0–6.0) ($N = 33$)
Inundation frequency (% of time)	15	30
NO_3 concentration (mmol m^{-3})	266 (105–558) ($N = 35$)	266 (26–487) ($N = 33$)

For salinity and NO_3, means, ranges and the number of observations are given.

vegetation (45–65% of the intertidal marsh surface). It has maximal dominance (65%) in the zone with mean salinity of about 6–7 PSU. As waters become more brackish (salinity >15 PSU) occurrences of reed are more fragmentary and constitute less than 1–2% of the vegetation. All in all, about 1.8 km^2, 33% of vegetated intertidal surface is covered by reed in the estuary, of which 80% below a salinity of 15 PSU. Most reed beds are located above mean high tidal level, and are submerged during spring tides. There is a tendency for reeds to occur deeper at lower salinity (Van Damme et al., 1999).

Two monospecific reed stands were intensively sampled for 3 years (1996–1999). Both vegetations were near to the water edge and regularly submerged (Table 1). Station Saeftinghe is located at the edge of Saeftinghe Marsh, and at the downstream limit of reed dominated vegetations. Here salinity varied seasonally between 4.5 and 20 PSU with a mean of 13.3 PSU. Station Burcht, in the oligohaline reach is located just south of Antwerp and salinity was always less than 6; average 1.6 PSU (Table 1). Nitrogen concentration near both sites was always high (Table 1). In February 1997, both reed beds were cut back and all litter removed.

Every month, six quadrants of 0.25 m^2, randomly chosen at least 1 m from the reed belt edge were harvested for aboveground biomass. Live and dead leaves and stems and panicles were separated and counted; the biomass was estimated after oven drying to constant weight and their C and N content was assessed. Dead biomass was only assessed in 1997. Data are standardized to 1 m^2 plots. On 17 September 1998, leaves from both stations were scanned for their total (single) surface area. These were subsequently dried and the specific leaf area (m^2 leaf g^{-1} leaf DW) was assessed by regression of leaf area (m^2) against leaf dry weight (g). In 1996, the root system was sampled five times using a stainless steel corer (diameter 7 cm), recovering the upper 30–100 cm. The living roots and rhizomes of six replicates were washed free of all sediment, dried in the oven to constant weight and their dry weight assessed.

Daily means of air temperature and solar radiation were obtained from a nearby weather station (Westdorpe). Total solar radiation was converted to photosynthetic active radiation (PAR) using a conversion factor of 0.5 (following Goudriaan and Van Laar, 1994).

1.2. Model setup

1.2.1. General description

The model describes the cycling of carbon mass (mol C m^{-2}) in a reed stand. It merges process descriptions from the reed model of (Asaeda and Karunaratne, 2000; hereafter denoted as AK2000) and the crop model Simple and Universal CROp Simulation (SUCROS; Penning de Vries and Van Laar, 1982; Goudriaan and Van Laar, 1994). Basically, the light harvesting and photosynthesis modelling and growth respiration was adopted from SUCROS; the other processes were patterned as in AK2000. All processes and associated parameters are listed in (Figs. 1 and 2) and (Tables 2–4).

The model distinguishes eight state variables: living roots, rhizomes, stems, leaves and panicles, dead leaves, stems and belowground organs (lump sum of dead roots and rhizomes; Fig. 1). The dynamics of modeled living organs is simple: all increase by a share of assimilates (growth); they loose a certain fraction of their mass by basal respiration or ageing and by mortality. Reallocation of mass may affect rhizomes, leaves and stems.

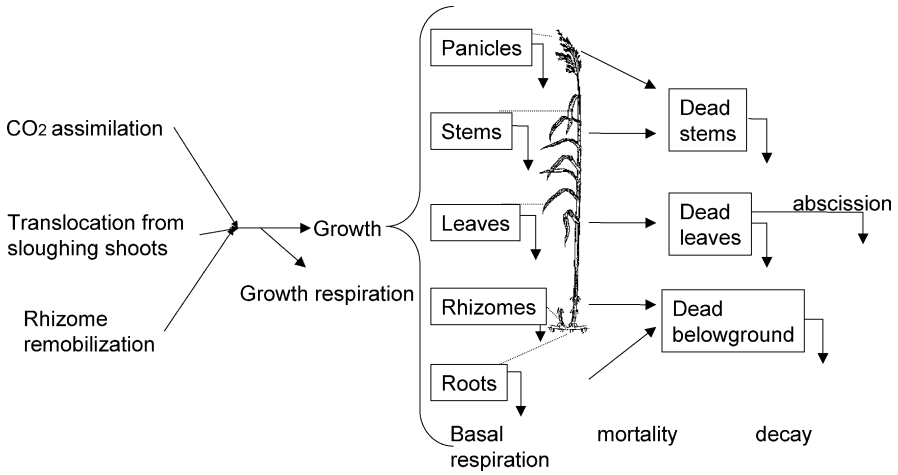

Fig. 1. Diagram of the model. Framed: modelled organs or carbon pools (dead and alive); other: modelled processes and rates.

Three source processes produce assimilates which are then distributed amongst the various organs where they serve to fuel growth. Distribution patterns are assumed to differ in different subsequent phenological phases (Fig. 2). The source processes are (1) photosynthesis (CO_2 assimilation), which takes place during the entire growing season, as soon as leaves are present, (2) remobilisation from rhizome biomass, which is triggered at the start of the growing season and proceeds till the end of the remobilisation phase and (3) reallocation of assimilates from leaves and stems, which commences at senescence.

Four demographic events are recognised: the start of growth (T1), the end of the rhizome remobilisation phase (T2), start of flowering (T3), and the start of senescence (T4). Shoot growth initiates in spring (T1) when the accumulated degree days above a 4 °C threshold exceed a critical (Tcrit) level (Goudriaan and Van Laar, 1994). The starting date of temperature accumulation was (artificially) set at 1 January, but the choice of 4 °C as a threshold value makes the model relatively insensitive to this date. The accumulated heat units at which tillers emerge were assessed by calibration and differ for both sites (see below). The other essential dates (T2, T3 and T4) are modelled independent of temperature but rather occur on fixed times of the year and are the same for each year. This is consistent with evidence that day length (possibly in interaction with low temperature) triggers reproduction and dormancy (Hay, 1990). They were also assessed by calibration. Remark that by fixing the date, the model cannot take into account the effects of temperature–day length interactions, or of a change of climate on its phenological timing, nor does it account for the significance of carbohydrate availability in the internal pool as a control on flowering (Clevering et al., 2001).

During the rhizome remobilisation phase, all assimilates are channelled in aboveground production. At the onset of senescence, assimilates are allocated to belowground organs (Fig. 2B). In-between, the allotment to belowground organs varies continuously, a description governed by one partitioning coefficient (ShapeBelow). Roots and rhizomes get a constant share of assimilates allocated to belowground organs (pRoots, 1-pRoots, parameter

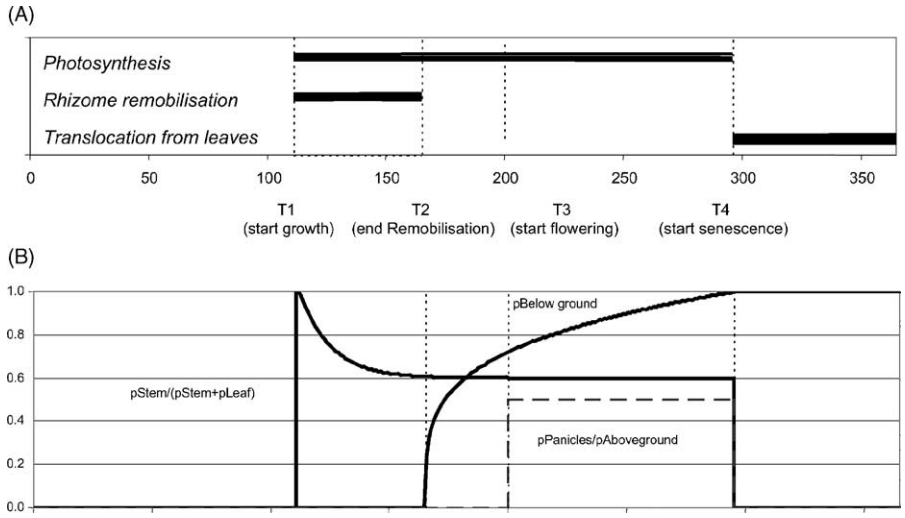

Fig. 2. Phenological events as implemented in the model. (A) The timing of four phenological events (T1–T4) and their impact on plant processes (rhizome remobilisation, photosynthesis and translocation from sloughing leaves). T2–T4 are fixed dates in all years, T1 depends on accumulated temperature as described in the text. (B) allocation strategy as a function of phenology. The fraction of assimilates allocated to roots and rhizomes as a function of day of the year (time) is estimated as:

$$\text{pBelowGround} = \left[\frac{\text{Time} - \text{T2}}{\text{T4} - \text{T2}}\right]^{\text{ShapeBelow}} \quad (\text{for Time} > \text{T2})$$

$$\text{pBelowGround} = 0 \quad (\text{Time} < \text{T2}).$$

A constant fraction (cRoot) of belowground matter is allocated to roots, a constant fraction (cPanicles) of aboveground assimilate (1−pBelowground) is allocated to panicles (dashed line):

$$\frac{\text{pPanicles}}{\text{pAboveGround}} = \text{cPanicles} \quad (\text{Time} > \text{T3}) .$$

The fraction of the remaining assimilate allocated to stems is estimated as:

$$\frac{\text{pStems}}{\text{pStems}+\text{pLeaves}} = \text{cLeaf} \times (1 - e^{(\text{Time}-\text{T1})\times \text{bL}}).$$

cRoot). The partitioning of aboveground matter takes into account the emergence of tillers at the start of the growing season. As these tillers are photosynthetically inactive, they are taken equivalent to stems in the model, and a function that decays exponentially with time (parameters bL, cLeaf) partitions assimilates between stems and leaves (Fig. 2B). At maturity (T3), certain shoots start to flower, and a fraction (pPanicles) of assimilate production is used for panicle formation (parameter cPanicles); the remainder being available to leaves and stems. All partitioning parameters were assessed by calibration.

1.2.2. Specific processes and parameters (Tables 2 and 3)

Air temperature influences the rates of processes according to the well-known Q_{10} concept (e.g. Čížková and Bauer, 1998; Arrhenius constant θ of 1.07); photosynthetically active radiation drives photosynthesis (Fig. 3).

Table 2
Model equations

Rates of change (mol C m^{-2} per day) of the state variables (mol C m^{-2})

$$\frac{dRhizomes}{dt} = rhizomeGrowth - rhizomeBasalRespiration - rhizomeMortality - rhizomeMobilisation$$

$$\frac{dRoots}{dt} = rootGrowth - rootBasalRespiration - rootMortality$$

$$\frac{dDeadBelowGround}{dt} = rootMortality + rhizomeMortality - belowgroundDecay$$

$$\frac{dLeaves}{dt} = leafGrowth - leafBasalRespiration - leafMortality - leafReallocation$$

$$\frac{dStems}{dt} = stemGrowth - stemBasalRespiration - stemMortality - stemReallocation$$

$$\frac{dPanicles}{dt} = panicleGrowth - panicleBasalRespiration - panicleMortality$$

$$\frac{dDeadleaves}{dt} = leafMortality - deadleavesDecay - deadleavesAbscission$$

$$\frac{dDeadstems}{dt} = stemMortality + panicleMortality - deadstemsDecay$$

Main processes (mol C m^{-2} per day)[a]

$RhizomeMobilisation = RemobilisationRate_{20} \cdot Rhizomes \cdot f(T)$

$OrganReallocation = ReallocationRate_{20} \cdot Organ \cdot f(T)$

$GlucoseProduction = Photosynthesis + RhizomeMobilisation + (leaf\ and\ stem)Reallocation$

$OrganGrowth = pOrgan \cdot GlucoseProduction \cdot (1 - RespFrac)$

$OrganBasalRespiration = RespirationRate_{20} \cdot Organ \cdot f(T)$

$OrganMortality = MortalityRate_{20} \cdot Organ \cdot f(T)$

$DeadOrganDecay = DecayRate_{20} \cdot DeadOrgan \cdot f(T)$

$DeadLeavesAbscission = AbscissionRate_{20} \cdot DeadLeaves \cdot f(T)$

Functions[b]

$f(T) = \theta^{(T-20)}$

Photosynthesis (mol C m^{-2} per day) $= \int_{x=0}^{x=\infty} P_{x,t} \cdot LAI \cdot dx$

$P_{x,t}$ (mol C m^{-2} leaf per day) $= Pmax_{20} \cdot f(T) \cdot (1 - \exp^{-I_{x,t} \cdot LUE / (Pmax_{20} \cdot f(T))})$

$I_{x,t}$ (W m^{-2} leaf) $= f(I_0, \rho, \lambda)$

LAI (m^2 leaf m^{-2} soil)$= SLA_C \cdot Leaves$

$Remobilisationrate_{20}$ (mol C m^{-2} per day)$= aRh \cdot Rhizomes^{bRh}$

[a] Organ is living leaves, stems, panicles, rhizomes or roots (mol C m^{-2}); DeadOrgan is dead leaves, stems, or belowground matter (mol C m^{-2}). pOrgan is the fraction of assimilates allocated to the respective organ, explained in Fig. 3. $Rate_{20}$ is the rate (per day) at 20 °C, $f(T)$ is the temperature function correcting the rates for the prevailing temperature (T, °C).

[b] θ is the Arrhenius constant. $P_{x,t}$ is the instantaneous gross CO_2 assimilation rate at depth x in the canopy per unit leaf surface; LAI is leaf area index. $I_{x,t}$ is the photosynthetically active radiation at depth x. It is calculated as a function of incident light (I_0, W m^{-2}), reflection of individual leaves (ρ) and extinction coefficient for diffuse radiation (λ) as in the model SUCROS (see text). $Pmax_{20}$ is the maximal assimilation rate per unit of leaf surface at 20 °C, LUE is the initial light use efficiency. SLA_C is the specific leaf area (m^2 mol C^{-1}).

Photosynthesis, the assimilation of CO_2 as carbohydrates using radiation as an energy source, is described as in the model SUCROS (Goudriaan and Van Laar, 1994). Gross CO_2 assimilation per unit of leaf surface ($P_{x,t}$) is calculated using absorbed radiation (a function of incoming radiation and crop leaf area) and the photosynthetic characteristic

Table 3
Parameter values

Parameter	Value
θ	1.07[a]
Tcrit (°days)	204 (Burcht), 300 (Saeftinghe)
T2 (stop rhizome remobilization) (days)	162
T3 (start panicles) (days)	199
T4 (start senescence) (days)	298
ShapeBelow (days)	0.36 (Burcht), 0.21 (Saeftinghe)
cRoot	0.08 (Burcht), 0.21 (Saeftinghe)
cPanicles	0.26 (Burcht), 0.26 (Saeftinghe)
cLeaf	0.33 (Burcht), 0.42 (Saeftinghe)
bL (per day)	−0.0625
$Pmax_{20}$ (mol C $(m^2 leaf)^{-1}$ per day)	2.0[b]
Eff (mol C $(W)^{-1}$ per day)	0.012
ρ	0.2[a]
λ $(m^2 leaf\ m^{-2} soil)^{-1}$	0.4[a]
SLA_C (m^2 leaf mol C^{-1})	0.42[c]
aRh	0.58[b]
bRh	−0.5[b]
$ReallocationRate_{20}$ (senescence) (per day)	0.18 (leaves), 0.0 (stems)[b]
$Respirationrate_{20}$ (per day)	0.002 (aboveground), 0.0018 (rhizomes), 0.0045 (roots)
RespFrac (mol C mol C^{-1})	0.25 (leaves), 0.16 (stems), 0.24 (panicles), 0.17 (belowground). See (Table 4) for details
$MortalityRate_{20}$ (growth phase) (per day)	0.0018 (stems), 0.0074 (leaves)
$MortalityRate_{20}$ (senescence) (per day)	0.1 (leaves, stems)
$MortalityRate_{20}$	0.00015[b] (belowground)
$AbscissionRate_{20}$	0.046 (leaves)
$DecayRate_{20}$	0.0025[b] (dead belowground), 0.006 (dead aboveground)

T2, T3 and T4 are time of phenological events; Tcrit is the critical accumulated temperature at which growth starts. ShapeBelow, cRoot and cPanicles, cLeaf and bL relate to the partitioning functions for assimilate, as explained in Fig. 3. Other parameters are explained in (Table 2).

[a] Values derived a priori from literature.

[b] Parameters fixed during the calibration.

[c] Measured.

The other parameters are derived by calibration. See text.

Table 4
Measured, average (±S.E.) C and N contents, calculated glucose requirements and respiration costs (RespFrac) as used in the model

	C (g C g DW^{-1})	N (g N g DW^{-1})	Glucose requirement (g Glucose g DW^{-1})	Respiration cost (mol C mol C^{-1})
Leaves ($N = 34$)	0.43 ± 0.010	0.035 ± 0.006	1.43	0.25
Stems ($N = 34$)	0.41 ± 0.010	0.018 ± 0.010	1.22	0.16
Panicles ($N = 18$)	0.45 ± 0.008	0.026 ± 0.007	1.49	0.24
Roots, rhizomes	0.43[a]	0.0125[a]	1.30	0.17

[a] From Rolletschek et al. (1999).

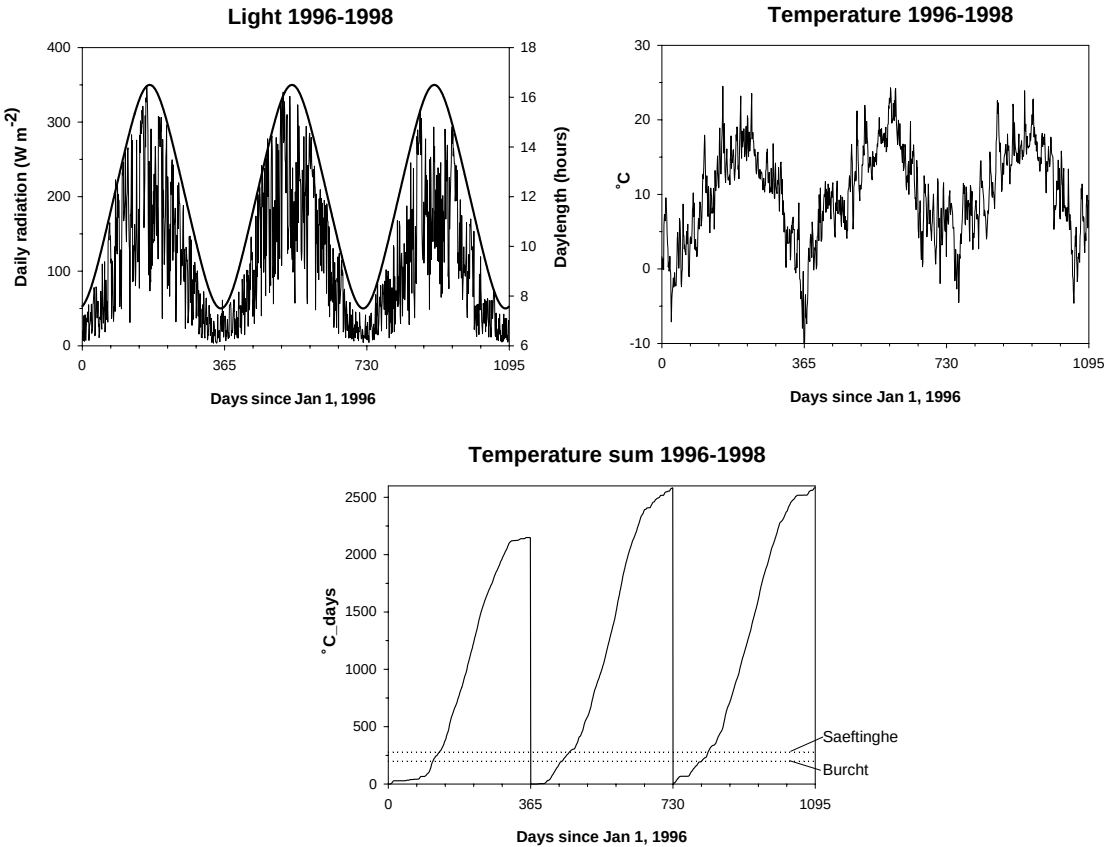

Fig. 3. Forcing functions. Above: meteorological characteristics of 1996–1998 driving the simulation. Left: light intensity (W m^{-2}) and day length (h; sine wave); Right: air temperature (°C). Below: Impact of temperature on emergence of *P. australis*: temperature sum (solid line) and critical value at which growth starts (dashed lines).

of single leaves (maximal photosynthesis rate $Pmax_{20}$, initial light use efficiency (LUE) coefficient), using a standard *P*/*I* curve. The five-points integration over canopy depth as in Goudriaan (1986) is used to calculate depth-integrated photosynthesis per unit of leaf area. The interception of light is formulated for a horizontally uniform stand of vegetation, assumes a spherical distribution of leaves and takes into account absorption of diffuse and direct radiation by sunlit and shaded leaves. The characteristics of the solar radiation (i.e. the diffuse and direct radiation) are calculated based on the latitude and day of the year, accounting for diurnal changes as in Goudriaan and Van Laar (1994). Taking into account the leaf area index (LAI), the total carbon assimilation by photosynthesis is then calculated.

The photosynthesis-light parameterisation is complete with a description of light absorption within the canopy. In the model SUCROS, light absorption is a function of the leaf area index and two parameters: a scattering coefficient of leaves for PAR (ρ, dimensionless) and an extinction coefficient for diffuse light (λ, m^2 soil surface m^{-2} leaf). The former was kept as in SUCROS (Goudriaan and Van Laar, 1994). The extinction coefficient λ was parameterised using a relationship between light absorbed and the leaf area index as derived for a reed stand SW of Paris by Allirand and Gosse (1995). Their best-fit equation was best reproduced with an extinction coefficient of 0.5 m^2 soil surface m^{-2} leaf. The leaf area index (m^2 leaf m^{-2} soil) was assessed by linear regression (see material and methods). As the intercept was not significant ($P = 0.42$), the regression was forced with zero intercept. Best fit gave: LAI = 0.015 leaf dry weight or 0.42 mol leaf carbon ($N = 53$; $r^2 = 0.97$).

The rhizome remobilisation rate depends on the rhizome biomass at the onset of growth, and is calculated with two coefficients (aRh, bRh) like in AK2000. At the onset of senescence, aboveground biomass is rapidly reallocated to belowground organs at a first-order rate. Basal respiration affects all organs and is also described using first-order kinetics. As in SUCROS, substantial respiration cost is associated to growth of each of the organs (such cost of biosynthesis was not included in the model of Asaeda and Karunaratne (2000)). The respiration cost for production of leaf, stem and panicle biomass (growth respiration, parameter respFrac) was calculated based on measured tissue composition and reported substrate carbon conversion efficiencies using the formulation of Vertregt and Penning de Vries (1987). Glucose requirement (*G*, g glucose g DW^{-1}) is expressed as a function of the carbon (C) and nitrogen (N) content (g g^{-1} DW) of the tissue to be made: $G = 5.4C + 6N - 1.1$. The corresponding respiration cost associated to growth (mol C respired for converting one mol C into structural biomass) can be calculated if C and N content of new biomass are known. Averaged C and N contents of the various organs and calculated glucose requirements and respiration costs are in (Table 4). The C and N content of rhizomes and roots were not measured, but we used mean values from Rolletschek et al. (1999). Note that the obtained respiration costs (0.17–0.25 mol C mol C^{-1}) compare well with reported respiration rates of 21% of fixed CO_2 in closed reed stands (Erdei et al., 2001).

Mortality of the various organs was modelled as a first-order process. In the reeds of the Scheldt estuary, shaded leaves close to the bottom senesce already during the growing season, after which they are shed and add to bottom litter. In addition, the ratio of living stems to total shoot biomass increases with time (see below) and this was taken as an indication that leaf mortality is larger than mortality of stems. Standing dead litter (leaves and stems) and dead belowground matter decline by decomposition, while dead leaves are also lost

by abscission. We imposed the same decay rates for leaves as for stems, but calibrated the abscission rate.

Finally, to include the changes induced by the differing salinity on the two reed stands, we assumed that salinity does not reduce performance of the plants on a leaf area basis (Adams and Bate, 1999; Rolletschek and Hartzendorf, 2000) but acts on reed morphology. Close inspection of the aboveground data revealed a difference in the timing of the start of growth in the two stands, so we also calibrated different thresholds of accumulated air temperature (Tcrit) to differentiate between both stations.

1.2.3. Model implementation

The model produces output from 1 January 1996 till 31 December 1998. This period is preceded by a spin-up period of 12 years, where the model is driven with a repeated seasonal cycle consisting of meteorological conditions of 1996–1998. In this way, the model results are effectively independent of the initial conditions, and we avoid estimating initial conditions of roots and rhizomes as extra parameters. Moreover, such recurrent simulations ensure that the carbon budget is balanced over a 3-year period. The model was implemented in FORTRAN in the simulation environment FEMME (Soetaert et al., 2002). It can be downloaded from http://www.nioo.knaw.nl/CEMO/FEMME.

1.2.4. Calibration, sensitivity analysis, validation

Model calibration and sensitivity analysis was performed according to the iterative procedure as explained in Brun et al. (2001). Here the most sensitive parameters are first selected, by calculating, for each parameter θ_j, the mean δ_j of the sensitivities $s_{i,j}$ of model output $\eta_i(\theta)$:

$$s_{i,j} = \frac{\Delta\theta_j}{\mathrm{SC}_i} \cdot \frac{\partial \eta_i(\theta)}{\partial \theta_j}$$

and

$$\delta_j = \sqrt{\frac{1}{n}\sum_{i=1}^{n} s_{i,j}^2}$$

where model output $\eta_i(\theta)$ is evaluated at the same points in time as the observations and for the current settings of the parameters (θ), n is the number of observations, $\Delta\theta_j$ a scaling value for parameter j, and SC_i the scaling for variable i. Large values of δ_j indicate large sensitivity of model output to the parameter j, zero sensitivity indicates that the parameter is not at all constrained by the data. After removing the least sensitive parameters, the near-linear dependence (so-called collinearity) of all possible parameter combinations is calculated. Parameter sets where collinearity exceeds the value 20 cannot be jointly estimated from the data, e.g. because the effect of changing one may be overruled by changes in the other parameter(s) (Brun et al., 2001). A parameter set that is 'identifiable' from the available data is then selected, the parameters calibrated and this procedure is repeated till convergence (see Brun et al., 2001 for more details). We used the Levenberg–Marquardt calibration algorithm to minimize the sum of squared residuals between model and data (Press et al., 1994; Soetaert et al., 2002). The parameter sensitivity functions $s_{i,j}$ were calculated with

the range of each parameter ($\Delta\theta_j$) set to 20% of its value, model observed variables were scaled (SC_i) with respect to the mean observed value.

The model was first calibrated to the data from the oligohaline station (Burcht) and subsequently verified on the mesohaline station (Saeftinghe).

2. Results

2.1. Biomass variation

Both inter-annual and inter-site variations in morphological characteristics are substantial (Table 5). Maximal shoot biomass was 30–100% higher in the oligo- compared to the mesohaline site and almost tripled in both stations from 1996 to 1997. Also, the shoot density was higher at the mesohaline station and increased strongly from 1996 to 1997. Panicle density and biomass was assessed in 1997. Only one-third of the shoots flowered at the oligohaline station Burcht and even less (15%) at Saeftinghe. In addition, reeds at the mesohaline station Saeftinghe had more, but smaller leaves and a somewhat higher leaf/stem ratio. The maximal biomass of leaf tissue was similar at both stations, but the stem biomass was much smaller at Saeftinghe.

The total rhizome-root system was of similar relative importance at both sites, but there were relatively more roots at Saeftinghe (15% versus 5% of total belowground biomass). Maximal biomass of rhizomes was 1.5 times that in the oligohaline reach, but mean biomass was comparable at both sites.

2.2. Model sensitivity, calibration, validation

Our model includes a total of 33 parameters. We fixed eight of these a priori based on literature data or our own measurements (see model setup, Table 4). A further six were

Table 5
Morphological characteristics of the two reed stands and in 3 subsequent years

	Station Saeftinghe			Station Burcht		
	1996	1997	1998	1996	1997	1998
Max density of shoots (m^{-2})	195	587	481	126	348	351
Max number of panicles (m^{-2})	NA	86	NA	NA	114	NA
Max stem biomass (g DW m^{-2})	395	766	1188	888	1242	1780
Max leaf biomass (g DW m^{-2})	224	410	490	278	433	420
Biomass of single leaf (g DW $leaf^{-1}$)	0.11	0.12	0.17	0.25	0.16	0.27
Max panicle biomass (g DW m^{-2})	NA	48	NA	NA	96	NA
Max total aboveground biomass[a] (g DW m^{-2})	587	1176	1678	1166	1664	2179
Max rhizome biomass (g DW m^{-2})	2391	NA	NA	3218	NA	NA
Mean rhizome biomass (g DW m^{-2})	1943	NA	NA	1933	NA	NA
Max root biomass (g DW m^{-2})	414	NA	NA	164	NA	NA
Max total belowground biomass (g DW m^{-2})	2806	NA	NA	3346	NA	NA

NA: not available.

[a] Ignoring panicles.

Table 6
Sensitivity of model output at station Burcht with respect to the parameters

Parameter	δ_j
T4	0.99
T2	0.35
T3	0.29
bRh[a]	0.27
Cleaf	0.26
LUE	0.25
Tcrit	0.10
$Pmax_{20}$[a]	0.09
$GrowthMortalityRate_{20}$ (leaves)	0.08
aRh[a]	0.07
ShapeBelow	0.06
$RespirationRate_{20}$ (rhizomes)	0.06
Cpanicles	0.05
$DecayRate_{20}$ (aboveground)	0.05
bL	0.05
$AbscissionRate_{20}$	0.05
$RespirationRate_{20}$ (aboveground)	0.04
PbelowToRoot	0.04
$RespirationRate_{20}$ (root)	0.04
$SenescenceMortalityRate_{20}$ (leaves, Stems)	0.03
$ReallocationRate_{20}$ (leaves)	0.02
$GrowthMortalityRate_{20}$ (stems)	0.02
$GrowthMortalityRate_{20}$ (belowground)[a]	<1e–2
$ReallocationRate_{20}$ (stems)[a]	<1e–6
$DecayRate_{20}$ (belowground)[a]	0.00

[a] Parameters removed from the calibration—see text for details.

given a fixed value before calibration and the remaining19 were left to be optimized during calibration (Table 3).

Table 6 shows the final sensitivity (δ_j) of the model output for station Burcht for all the 25 parameters that had not been assigned an a priori value. The parameters are ranked according to decreasing sensitivity. The model was found to be most sensitive to the timing of phenological events, i.e. the cessation of rhizome remobilization (T2), the onset of flowering (T3) and senescence (T4), and less to the onset of growth (Tcrit). In addition, the outcome of the model was also highly affected by the rhizome remobilization (bRh) and photosynthesis rate (both LUE and $Pmax_{20}$). In contrast, the decay rate of belowground detrital matter was not constrained at all by the data ($\delta_j^{msqr} = 0$), whilst the model output was only marginally sensitive to the belowground mortality and the stem reallocation rate (very low values of δ_j^{msqr}). These three parameters were first removed from the calibration analysis, and their values fixed. Belowground mortality rates were set the same as in AK2000. Dead roots decay on average 0.0025 per day (0.0014–0.0032 per day, Wrubleski et al., 1997; Ibanez et al., 1999), a value taken as indicative for total belowground decay rate. Stem reallocation rate at senescence was set to 0 per day.

Considerable collinearity between the two coefficients relating to rhizome remobilization rate (aRh and bRh; collinearity >500) and between maximal photosynthesis rate

($Pmax_{20}$) and the light use efficiency (15.5) suggested that parameter combinations containing these parameter pairs would be difficult to identify from the data. This was solved as follows: (1) for calculating the rhizome remobilization, the values of aRh and bRh were imposed as in AK2000. (2) Maximal net CO_2 assimilation rates range within 6–27 μmol CO_2 m^{-2}leaf s^{-1} (Overdieck and Raghi-Atri, 1976; Lissner et al., 1999; Erdei et al., 2001; Lessmann et al., 2001). Using a growth efficiency of 75%, we calculate a maximal photosynthesis rate of about 0.7–3.1 mol C m^{-2} leaf per day. We imposed $Pmax_{20}$ to the mean value 2.0 mol C m^{-2} leaf per day and estimated the value of the light use efficiency parameter by calibration. The collinearity index of the remaining 19 parameters was 17.7, which is sufficiently small to allow estimating them all at once by automatic calibration.

Initially these parameters were allowed to vary freely (i.e. no constraints on upper or lower bounds). In the absence of restrictions however, the three basal respiration rates tended to become almost 0, so they were not allowed to decrease more than 10% of preset values. Initial rhizome respiration rates (0.002 per day) were taken from Čížková and Bauer (1998). Root respiration was set somewhat higher than rhizome respiration, to account for the energetic cost associated with nutrient uptake; initial values (0.005 per day) were the same as in Asaeda et al. (2002). These rates are an order of magnitude smaller than root respiration rates observed for seedlings by Romero et al. (1999). Shoot respiration was initially set to a low value of 0.0025 per day. After calibration, all these values were at the lower limit of the range.

The calibrated values from the 16 parameters that had been allowed to vary freely remained well within ranges reported from the literature or from the model of Asaeda and Karunaratne (2000). Lessmann et al. (2001) report an apparent quantum efficiency ranging from 0.022 to 0.046 mol CO_2 (mol photons)$^{-1}$. Using a conversion of 4.2 μmol photons J^{-1} this corresponds to a light use efficiency (LUE) of 0.008–0.017 mol C W^{-1} per day. The calibrated value was 0.012 mol C W^{-1} per day. Using the regression of date of flowering versus latitude from Clevering et al. (2001), we deduced a typical start of panicle formation at day 200, similar to the calibrated value (T3 = day 199). During the growth phase, aboveground mortality was 0.003 per day in AK2000, but this was an average value for combined stems and leaves. As the model was constrained to reproduce the observed change in stem/shoot ratio, higher mortality of leaves compared to stems ensued. The best fit was achieved with a mortality rate (at 20 °C) of 0.0018 per day for stems, 0.0074 per day for leaves. With stems accounting from 60 to 100% of shoot biomass, this corresponds to a shoot mortality varying within 0.002–0.004 per day, embracing the average shoot mortality from the model of AK2000. First-order decay rates of dead culms and/or sheaths were compiled in Gessner (2001) and range from 0.0004 to 0.005 per day; average 0.002 per day; dead leaves decay at a higher rate ranging between 0.0009 and 0.009 per day, average of 0.004 per day (Gessner, 2001; Akanil and Middleton, 1997; Menendez et al., 2001). The mean decay rate of leaves and stems (at 20 °C) obtained after calibration was 0.006 per day, which gives an effective decomposition rate of 0.002–0.003 per day at the prevailing temperature (most of the decay occurs during winter).

After calibration of the 19 parameters to the data from oligohaline station Burcht, the model was verified based on the data for mesohaline station Saeftinghe. This was done by recalibrating the model to the data from Saeftinghe, keeping the 33 parameter values as derived from Burcht, except for five parameters that were assumed to represent the effect

Table 7
Annual mean (±S.E.) meteorological conditions of the 3 years ($N = 365$)

	Daily solar radiation ($W\,m^{-2}$)	Temperature (°C)
1996	115 ± 89	8.9 ± 6.6
1997	120 ± 90	10.6 ± 6.3
1998	105 ± 82	10.7 ± 5.7

of the growth site. These parameters were chosen to be consistent with the observations that the growth site affects reed morphology (see above) and that growth started later at station Saeftinghe. Four parameters relate to the allocation of resources to different organs (parameters ShapeBelow, cRoot, cLeaf, cPanicles), and the fifth was the critical accumulated degree days that trigger growth initiation (Tcrit). Resulting parameter values for station Saeftinghe deviated strongly with respect to the initiation of growth (Tcrit changed from 204°days for Burcht to 300°days for Saeftinghe), and with respect to the partitioning of assimilates towards belowground matter (ShapeBelow from 0.08 to 0.21) or towards roots (cRoot from 0.36 to 0.21) and between leaves and stems (cLeaf from 0.33 to 0.42). However, the share of assimilates allotted to panicles (cPanicles) was not altered during the calibration.

The equilibrium biomass of belowground organs and the variation between years and between the stations of aboveground biomass is largely reproduced by the model (Fig. 4). Differences in weather conditions in spring, by their effect on the emergence of tillers have reproduced most of the interannual variation, whereas the imposed difference in the timing of growth initiation is the main factor explaining divergence in biomass between the stations. The meteorological characteristics of 1996–1998 that drive the model's dynamics are in Fig. 3 and the mean for each year is in (Table 7). All years were quite comparable with respect to mean solar radiation and mean temperature. However, winter–spring in 1996 was markedly colder than the other years. This is best viewed by comparing the accumulated temperature, above the threshold temperature 4 °C (which triggers growth), for the three years as resulting from the model (Fig. 3 lower). As weather was much more favourable for the development of buds on the rhizomes in spring of 1997 and 1998 growth started about one month earlier than in 1996. The critical threshold of accumulated degree days in the model was attained on 24 April 1996, 22 March 1997, 15 March 1998, at the oligohaline site (Burcht) and about 3 weeks later at Saeftinghe (15 May 1996, 15 April 1997, 2 April 1998) (Fig. 3).

Some disparities between model and data exist. At the mesohaline station for instance, there is a tendency to overestimate stem biomass in 1996, and to underestimate it in 1998, whereas the leaf biomass is much better reproduced. To a lesser extent the same defect also applies to the oligohaline station. This divergence between observed and predicted behaviour is more clearly visualized by close inspection of the stem to shoot ratio (Fig. 5). The data demonstrate a gradual increase of this ratio from 1996 till 1998, most prominent for the mesohaline station, but this has not been captured by the model. As the possible reasons for this behaviour are not clear, we decided not to improve performance by imposing such a temporal trend. It is however noteworthy to see that, although the model may miss the differences amongst years in the stem/shoot ratio, it reproduces quite faithfully the subtle seasonal changes. The drop in stem/shoot fraction at the onset of growth is imposed by

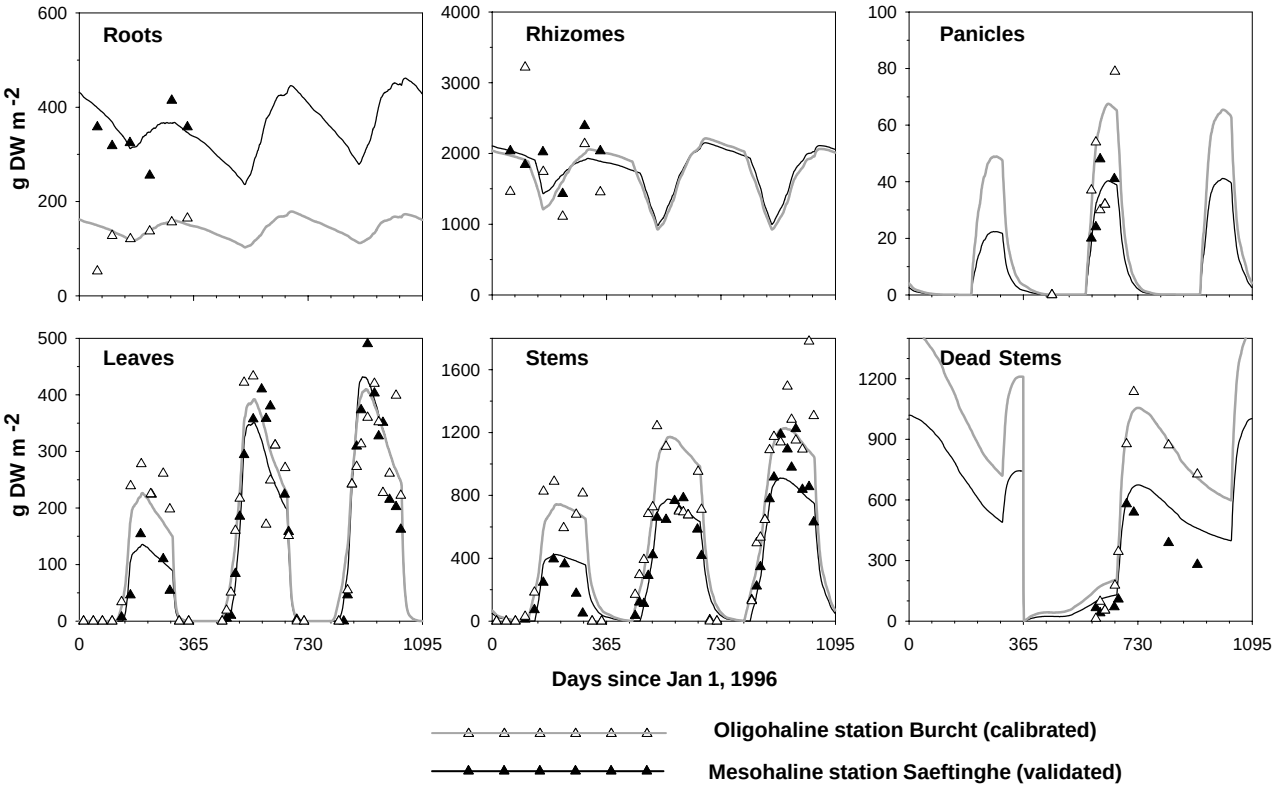

Fig. 4. Observed and modelled quantities at the two stations for the period 1996–1998. Units in gram ash free dry weight m^{-2} were converted from the model units (mol C m^{-2}) using the conversion factors of Table 4.

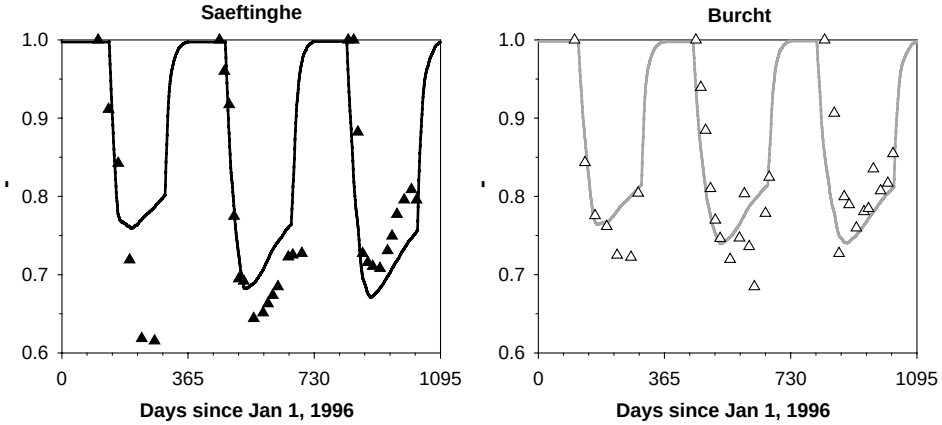

Fig. 5. Fraction of stems in shoots (modelled and observed) for mesohaline station Saeftinghe (left) and oligohaline station Burcht (right).

the function (Fig. 2) that partitions assimilates between stems and leaves, mimicking tiller emergence, but the increase towards the end of the growing season results from imposing the higher mortality rate of leaves compared to stems.

2.3. Carbon budget

Photosynthetic production is slightly higher in the oligohaline (121 mol C m^{-2} per year), compared to the mesohaline station (105 mol C m^{-2} per year; Fig. 6). It is by far the most dominant process contributing to assimilate production (78–80%). Next comes remobilisation from rhizomes (28 and 23 mol C m^{-2} per year at oligo- and mesohaline station, respectively). The resorption of carbon from leaves is almost negligible (5 and 4 mol C m^{-2} per year, respectively), notwithstanding the high resorption rate in the model at senescence. This is in sharp contrast to the results of Asaeda and Karunaratne (2000), where this process amounts to about 25% of net photosynthetic production. We disregarded resorption from non-senescing leaves in the active growth phase, whereas Asaeda and Karunaratne (2000) did include this process. From the data, we cannot distinguish whether the increase of leaf tissue results from direct allocation of assimilates (as in our model) or as the net effect of allocation and resorption. By short-circuiting resorption during the growth phase we may have made leaf growth more efficient than in reality. However, it has been argued that, as resorption reduces the loss of elements, it is relatively unimportant for reeds growing in nutrient-rich conditions (Boar, 1996; Lippert et al., 1999), such as in the Scheldt estuary.

Some 82% of gross production is used for growth, and allocated to the various organs. An important part of the excess energy acquired by photosynthesis is stored in the rhizome-root system, probably to allow rapid initial growth in spring. In addition, energy is needed to fulfill maintenance costs of roots and rhizomes. Thus, 45 and 54% of all assimilates flow back towards the rhizome-root system during active growth, at the oligo- and mesohaline station.

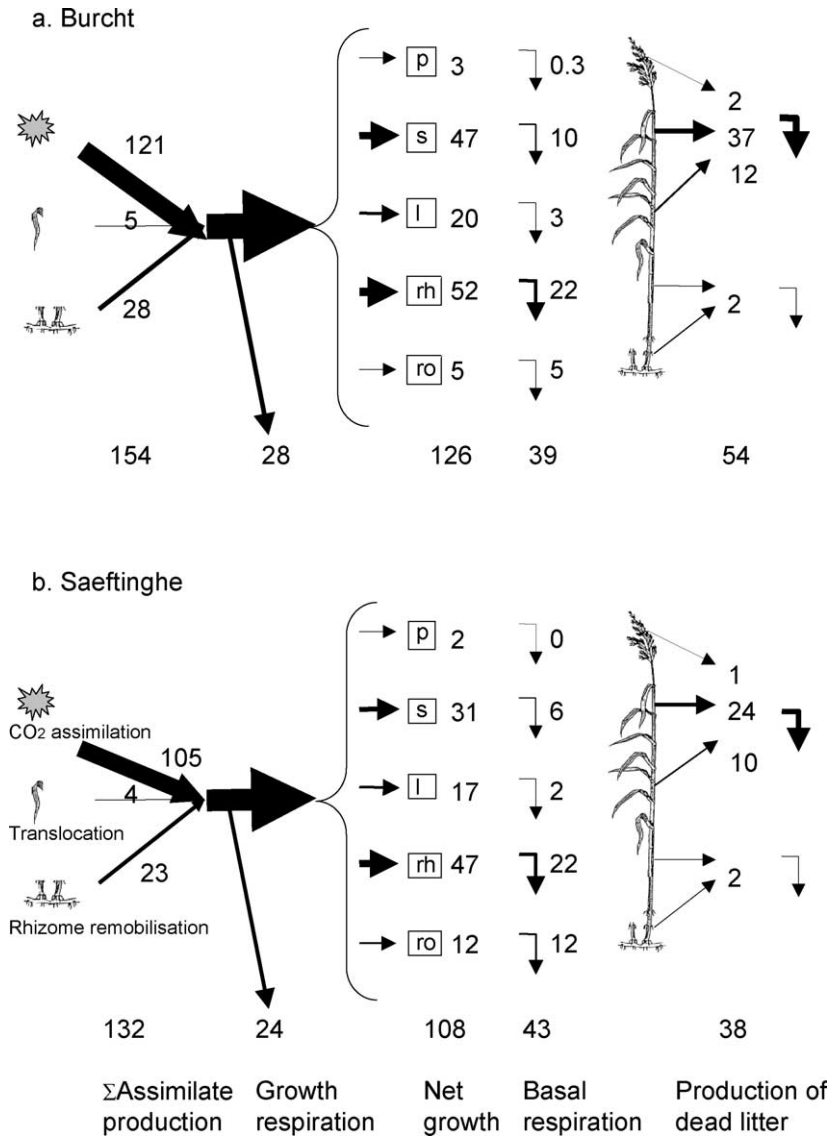

Fig. 6. Annual carbon budget (average of 1996–1998) of the reed stand at oligohaline station Burcht (above) and Saeftinghe (below). Flows in mol C m^{-2} per year. To convert to DW, use C content of the tissues in Table 4.

Roots get a share equal to 9% (oligo) and 25% (mesohaline station) of these belowground assimilate flows.

The photosynthetic production creates new biomass, which, in a balanced budget is compensated by external losses. In the model, the largest part of this new (gross) production fuels respiration, either to provide the energy for growth (23%) or to pay maintenance costs such as to maintain the metabolic integrity of the plant (33% at the oligo-, 41% at the

mesohaline station). Similarly high maintenance costs were found in the simulations of Asaeda and Karunaratne (2000). The larger maintenance costs at the mesohaline station are caused by the higher preponderance of roots here. The remaining 44% (oligohaline) and 36% (mesohaline) of new assimilates produced by photosynthesis accumulates as dead litter and is ultimately mineralized by the external ecosystem. Some 55% of these assimilates are used for aboveground biomass at the oligohaline, 45% at the mesohaline station. Roots get a much lower share (5 mol C m^{-2} per year compared to 12 mol C m^{-2} per year), whilst production of stems is higher at Burcht compared to Saeftinghe (47 and 31 mol C m^{-2} per year). Consequently more dead litter is produced at the oligohaline station (54 mol C m^{-2} per year compared to 38 mol C m^{-2} per year).

3. Discussion

The model that was developed here synthesizes how weather (temperature and solar radiation) acts through the life history, resource allocation and the modulation of rates, to direct the standing stock and productivity of two reed beds in the Scheldt estuary. It shares many features with a reed model that was developed previously (Asaeda and Karunaratne, 2000), but describes a more complete set of organs which, except for dead belowground biomass, have all been measured in the field. A large number (19) of parameter values could be simultaneously assessed from the data obtained from one site (oligohaline station Burcht) indicating that, although the measurements consisted solely of biomasses, a great deal of process information can be extracted from such data. Calibrated rate values were either consistent with measurements or with the model of Asaeda and Karunaratne (2000) suggesting that they are more generally applicable. Application of the model to a second site (mesohaline station Saeftinghe) required adaptation of four parameters only, dealing with resource allocation and timing of growth initiation. As the agreement between model predictions and field data is quite satisfactory, we used the model to hindcast the processes driving the dynamics of the reed beds and to explain the temporal and inter-site variation.

3.1. Reed biomass

The two sites described here are most strongly discriminated by the salinity regime of the water. The reed stand at Saeftinghe (mean salinity 13.3 PSU) grows most likely at the edge of its physiological tolerance. In contrast, at Burcht, waters are less saline (mean salinity 1.6 PSU), offering more optimal conditions for growth (Hartzendorf and Rolletschek, 2001). Notwithstanding these different growth conditions, reeds at both sites were healthy and shared several features with other stands growing in temperate, nutrient-rich environments (Table 5). They were characterised by large shoot density (126–587 m^{-2}), high productivity and standing stock of both aboveground (587–2659 g DW m^{-2}) and belowground biomass (2806–3346 g DW m^{-2}), low reproductive fertility (fraction of panicle-bearing culms between 15 and 33%) and had a similar chemical composition (e.g. C:N ratios, Table 4) indicative of eutrophic growth conditions (e.g. Kohl et al., 1998; Lippert et al., 1999).

The two reed stands did however differ from each other in several ways. At the mesohaline station Saeftinghe, shoot densities were consistently higher, shoots and leaves smaller,

and maximal aboveground and belowground biomasses lower. Although the aboveground–belowground ratio was similar in the two sites (∼0.7), roots were more prominent (14.7% against 4.8% of belowground biomass) at the mesohaline station. Except for shoot density, these dissimilarities compare well with responses to stress factors reported in other studies, e.g. salinity (Rolletschek and Hartzendorf, 2000; Mauchamp and Mesleard, 2001) or low habitat fertility (Kühl et al., 1997; Lippert et al., 1999; Hardej and Ozimek, 2002). The tendency for stressors to affect shoot density is not as clear: density tends to decrease as a response to nutrient shortage, to increase in response to cutting (Ostendorp, 1999), after herbivory (van den Wyngaert et al., 2003) or shading (Ekstam, 1995) but may increase (Hanganu et al., 1999, this study), decrease (Hellings and Gallagher, 1992) or any effect may be lacking (Mauchamp and Mesleard, 2001) in response to higher salinity (or another, related factor).

Standing stocks of aboveground organs also showed significant variation between years, with biomass in 1998 almost twice that of 1996. The model suggests that differences in the timing of bud burst in spring are mainly responsible for both the inter-site and inter annual variation. In 1996, growth initiation was retarded with about 1 month compared to subsequent years, caused by lower spring temperatures, and consequently maximal biomass was much lower. Interestingly, budding of the plants in the mesohaline site was also delayed with about 3 weeks compared to the oligohaline site and including this explained the lower biomass in the mesohaline site.

Unfortunately, the reed beds in the Westerschelde were cut back in winter 1996–1997 and litter was removed, which coincided with the change in weather conditions. Because of that we cannot decide whether the faster growth initiation in 1997 and 1998 was caused by differences in weather (as resulting from the model) or by this management measure. Nevertheless, dependence of summer standing crop on timing of emergence of shoots has been observed in other studies, albeit in a different context, i.e. as a response to increased nutrient availability (Lippert et al., 1999; Hardej and Ozimek, 2002) or as a function of latitude (Clevering, 1999; Clevering et al., 2001).

3.2. Carbon budget

At both sites, photosynthesis contributed most to total reed growth, with a share of 78–80%, and followed by remobilisation from rhizomes (17–19%), whilst the resorption of carbon from leaves was almost negligible (3%). About 50% of all assimilates were channelled to belowground organs, and this agrees with previous estimates of the ratio of aboveground to belowground production in *P. australis*, varying between 0.34 and 1.4 (Westlake, 1982).

Although the differences in resource allocation and timing of growth initiation in the two reed beds have a pronounced effect on aboveground biomass, the impact on total production and on the fate of this production was smaller. In the model the maximal aboveground biomass is about 50% higher at the oligohaline station, but photosynthesis was only 17% larger. On the one hand, the negative impact of retarded growth initiation in the mesohaline station is partly counteracted by the higher allocation to leaf tissue, which tends to increase growth. Hence the similar net growth despite the dissimilar total aboveground biomass in the two sites. On the other hand, the higher allocation of assimilates to roots in the

mesohaline station must have increased the maintenance costs (33% of new photosynthetic production at the oligo-, 41% at the mesohaline station) at the expense of the accumulation of biomass, hence the differences in aboveground biomass despite the similarity in growth. Consequently a smaller share of net production accumulates as detritus in the mesohaline station (36% versus 44%).

Comparing the flow of assimilates with maximal standing stocks, we calculate an annual turnover of 60–65% for rhizomes, 72–74% for roots, and 100% for aboveground biomass.

4. Conclusion

The overall picture that emerges from the matching of field data from the Scheldt estuary and the model is that much of the variability in reed biomass and production relates to the timing of bud burst in spring. In 1996, a year with unfavourable weather in winter and spring, growth initiation was retarded and this had a pronounced effect on maximal biomass reached in summer, about 50% lower than the following years. In addition, our results suggest that high salinity or perhaps some other, related factor similarly affected the reed bed in the mesohaline site, by postponing growth initiation by several weeks. This led to a shorter growing season and consequently total production and maximal biomass was reduced compared to reeds growing in the oligohaline site.

Acknowledgements

The authors thank the KNMI for providing the meteorological data. This study was carried out within the OMES project, supported by the Flemish community, Belgium. The model can be downloaded from the FEMME website (http://www.nioo.knaw.nl/CEMO/FEMME) or is available upon request. This is publication nr 3276 from the NIOO.

References

Adams, J.B., Bate, G.C., 1999. Growth and photosynthetic performance of *Phragmites australis* in estuarine waters: a field and experimental evaluation. Aquat. Bot. 64, 359–367.

Akanil, N., Middleton, B., 1997. Leaf litter decomposition along the Porsuk River, Eskisehir Turkey. Can. J. Bot. 75, 1394–1397.

Allirand, J.-M., Gosse, G., 1995. An above-ground biomass production model for a common reed (*Phragmites communis* Trin) stand. Biomass Bioenergy 9, 441–448.

Asaeda, T., Karunaratne, S., 2000. Dynamic modeling of the growth of *Phragmites australis*: model description. Aquat. Bot. 67, 301–318.

Asaeda, T., Nam Le, H., Hietz, P., Tanaka, N., Karunaratne, S., 2002. Seasonal fluctuations in live and dead biomass of *Phragmites australis* as described by a growth and decomposition model: implications of duration of aerobic conditions for litter mineralisation and sediment. Aquat. Bot. 73, 223–239.

Boar, R.R., 1996. Temporal variations in the nitrogen content of *Phragmites australis* (Cav) Trin ex Steud from a shallow fertile lake. Aquat. Bot. 55, 171–181.

Boschker, H.T.S., Dekkers, E.M.J., Pel, R., Cappenberg, T.E., 1995. Sources of organic carbon in the littoral of lake Gloomier as indicated by stable carbon-isotope and carbohydrate compositions. Biogeochemistry 29, 89–105.

Brix, H., Sorrell, B.K., Lorenzen, B., 2001. Are *Phragmites*-dominated wetlands a net source or net sink of greenhouse gases? Aquat. Bot. 69, 313–324.

Brun, R., Reichert, P., Künsch, H., 2001. Practical identifiability analysis of large environmental simulation models. Water Resour. Res. 37, 1015–1030.

Burdick, D.M., Buchsbaum, R., Holt, E., 2001. Variation in soil salinity associated with expansion of *Phragmites australis* in salt marshes. Envirn. Exp. Bot. 46, 247–261.

Chambers, R.M., 1997. Porewater chemistry associated with *Phragmites* and *Spartina* in a Connecticut tidal marsh. Wetlands 17, 360–367.

Čížková, H., Bauer, V., 1998. Rhizome respiration of *Phragmites australis*: effect of rhizome age, temperature, and nutrient status of the habitat. Aquat. Bot. 61, 239–253.

Clevering, O.A., 1999. Between- and within-population differences in *Phragmites australis*. 1. The effects of nutrients on seedling growth. Oecologia 121, 447–457.

Clevering, O.A., Brix, H., Lukavská, J., 2001. Geographic variation in growth responses in *Phragmites australis*. Aquat. Bot. 69, 89–108.

Coops, H., Boeters, R., Smit, H., 1991. Direct and indirect effects of wave attack on helophytes. Aquat. Bot. 41, 333–352.

Coops, H., Van den Brink, F.W.B., Van der Velde, G., 1996. Growth and morphological responses of four helophyte species in an experimental water-depth gradient. Aquat. Bot. 54, 11–24.

Ekstam, B., 1995. Ramet size equalization in a clonal plant, *Phragmites australis*. Oecologia 104, 440–446.

Erdei, L., Horváth, F., Tari, I., Pécsváradi, A., Szegletes, Z., Dulai, S., 2001. Differences in photorespiration, glutamine synthetase and polyamines between fragmented and closed stands of *Phragmites australis*. Aquat. Bot. 69, 165–176.

Gessner, M.O., Schieferstein, B., Muller, U., Barkmann, S., Lenfers, U.A., 1996. A partial budget of primary organic carbon flows in the littoral zone of a hardwater lake. Aquat. Bot. 55, 93–105.

Gessner, M.O., 2001. Mass loss, fungal colonisation and nutrient dynamics of *Phragmites australis* leaves during senescence and early aerial decay. Aquat. Bot. 69, 325–339.

Goudriaan, J., Van Laar, H.H., 1994. Modelling potential crop growth processes. Textbook with exercises. Current issues in production ecology, vol. 2. Kluwer, Dordrecht. 238 pp.

Goudriaan, J., 1986. A simple and fast numerical method for the computation of daily totals of crop photosynthesis. Agric. Forest Meteorol. 38, 251–255.

Hanganu, J., Mihail, G., Coops, H., 1999. Responses of ecotypes of *Phragmites australis* to increased seawater influence: a field study in the Danube Delta, Romania. Aquat. Bot. 64, 351–358.

Hardej, M., Ozimek, T., 2002. The effect of sewage sludge flooding on growth and morphometric parameters of *Phragmites australis* (Cav.) Trin. ex Steudel. Ecol. Eng. 18, 343–350.

Hartzendorf, T., Rolletschek, H., 2001. Effects of NaCl-salinity on amino acid and carbohydrate contents of *Phragmites australis*. Aquat. Bot. 69, 195–208.

Hay, R.K.M., 1990. Tansley review no 26. The influence of photoperiod on the dry-matter production of grasses and cereals. New Phytol. 116, 233–254.

Hellings, S.E., Gallagher, J.L., 1992. The effects of salinity and flooding on *Phragmites australis*. J. Appl. Ecol. 29, 41–49.

Hootsmans, M.J.M., Wiegman, F., 1998. Four helophyte species growing under salt stress: their salt of life? Aquat. Bot. 62, 81–94.

Ibanez, C., Day, J.W., Pont, D., 1999. Primary production and decomposition of wetlands of the Rhone delta. France: interactive impacts of human modifications and relative sea level rise. J. Coast. Res. 15, 717–731.

Karunaratne, S., Asaeda, T., 2000. Verification of a mathematical growth model of *Phragmites australis* using field data from two Scottish lochs. Folia Geobot. 35, 419–432.

Klimes, L., Klimesova, J., Čížková, H., 1999. Carbohydrate storage in rhizomes of *Phragmites australis*: the effects of altitude and rhizome age. Aquat. Bot. 64, 105–110.

Kohl, J.G., Woitke, P., Kühl, H., Dewender, M., Konig, G., 1998. Seasonal changes in dissolved amino acids and sugars in basal culm internodes as physiological indicators of the C/N-balance of *Phragmites australis* at littoral sites of different trophic status. Aquat. Bot. 60, 221–240.

Kühl, H., Kohl, J.G., 1992. Nitrogen accumulation, productivity and stability of reed stands (*Phragmites australis* (Cav) Trin Ex Steudel) at different lakes and sites of the lake districts of Uckermark and Mark Brandenburg (Germany). Intern. Rev. Ges. Hydrobiol. 77, 85–107.

Kühl, H., Woitke, P., Kohl, J.G., 1997. Strategies of nitrogen cycling of *Phragmites australis* at two sites differing in nutrient availability. Int. Rev. Hydrobiol. 82, 57–66.

Lessmann, J.M., Brix, H., Bauer, V., Clevering, O.A., Comín, F.A., 2001. Effect of climatic gradients on the photosynthetic responses of four *Phragmites australis* populations. Aquat. Bot. 69, 109–126.

Lippert, I., Rolletschek, H., Kühl, H., Kohl, J.G., 1999. Internal and external nutrient cycles in stands of *Phragmites australis*—a model for two ecotypes. Hydrobiologia 409, 343–348.

Lissner, J., Schierup, H.H., 1997. Effects of salinity on the growth of *Phragmites australis*. Aquat. Bot. 55, 247–260.

Lissner, J., Schierup, H.H., Comín, F.A., Astorga, V., 1999. Effect of climate on the salt tolerance of two *Phragmites australis* populations. I. Growth, inorganic solutes, nitrogen relations and osmoregulation. Aquat. Bot. 64, 317–333.

Mauchamp, A., Mesleard, F., 2001. Salt tolerance in *Phragmites australis* populations from coastal Mediterranean marshes. Aquat. Bot. 70, 39–52.

Menendez, M., Martinez, M., Hernandez, O., Comín, F.A., 2001. Comparison of leaf decomposition in two Mediterranean rivers: a large eutrophic river and an oligotrophic stream (S Catalonia, NE, Spain). Int. Rev. Hydrobiol. 86, 475–486.

Ostendorp, W., 1999. Management impacts on stand structure of lakeshore *Phragmites* reeds. Int. Rev. Hydrobiol. 84, 33–47.

Ostendorp, W., Tiedge, E., Hille, S., 2001. Effect of eutrophication on culm architecture of lakeshore *Phragmites* reeds. Aquat. Bot. 69, 177–193.

Overdieck, D., Raghi-Atri, F., 1976. CO_2-netto-assimilation von *Phragmites australis* (Cav.) Trin. Ex Steud. Blattern bei unterschiedlichen Mengen an Stickstof und Phosphor im Nährsubstrat. Angew. Botanik 50, 267–283.

Penning de Vries, F.W.T., Van Laar, H.H., 1982. Simulation of plant growth and crop production. Simulation monographs, Pudoc, Wageningen, 308 pp.

Press, W.H., Teukolsky, S.A., Vetterling, W.T., Flannery B.P., 1994. Numerical Recipes in Fortran, second ed. Cambridge University Press, Cambridge, 963 pp.

Rolletschek, H., Hartzendorf, T., 2000. Effects of salinity and convective rhizome ventilation on amino acid and carbohydrate patterns of *Phragmites australis* populations in the Neusiedler Sea region of Austria and Hungary. New Phytol. 146, 95–105.

Rolletschek, H., Rolletschek, A., Kühl, H., Kohl, J.G., 1999. Clone specific differences in a *Phragmites australis* stand II. Seasonal development of morphological and physiological characteristics at the natural site and after transplantation. Aquat. Bot. 64, 247–260.

Romero, J.A., Brix, H., Comín, F.A., 1999. Interactive effects of N and P on growth, nutrient allocation and NH_4 uptake kinetics by *Phragmites australis*. Aquat. Bot. 64, 369–380.

Sanchez, J.M., Otero, X.L., Izco, J., 1998. Relationships between vegetation and environmental characteristics in a salt-marsh system on the coast of Northwest Spain. Plant Ecol. 136, 1–8.

Soetaert, K., Herman, P., 1995. Nitrogen dynamics in the Westerschelde estuary (S.W. Netherlands) estimated by means of the ecosystem model MOSES. Hydrobiologia 311, 225–246.

Soetaert, K., deClippele, V., Herman, P., 2002. Femme, a flexible environment for mathematically modelling the environment. Ecol. Model. 151, 177–193.

Squires, L., Van der Valk, A.G., 1992. Water-depth tolerances of the dominant emergent macrophytes of the delta Marsh, manitoba. Can. J. Bot. 70, 1860–1867.

Van Damme, S., Ysebaert, T., Meire, P., Van de Bergh, E., 1999. Habitatstructuren, waterkwaliteit, en leefgemeenschappen in het Schelde-estuarium. Rapport Instituut voor Natuurbehoud 99/24, Brussel (in Dutch).

van den Wyngaert, I.J.J., Wienk, L.D., Sollie, S., Bobbink, R., Verhoeven, J.T.A., 2003. Long-term effects of yearly grazing by moulting Greylag geese (Anser anser) on reed (*Phragmites australis*) growth and nutrient dynamics. Aquat. Bot. 75, 229–248.

Van der Nat, F.J., Middelburg, J.J., 2000. Methane emission from tidal freshwater marshes. Biogeochemistry 49, 103–121.

Van der Putten, W.H., 1997. Die-back of *Phragmites australis* in European wetlands: an overview of the European research programme on reed die-back and progression (1993–1994). Aquat. Bot. 59, 263–275.

Vertregt, N., Penning de Vries, F.W.T., 1987. A rapid method for determining the efficiency of biosynthesis of plant biomass. J. Theor. Biol. 128, 109–119.

Vretare, V., Weisner, S.E.B., Strand, J.A., Granéli, W., 2001. Phenotypic plasticity in *Phragmites australis* as a functional response to water depth. Aquat. Bot. 69, 127–145.

Weisner, S.E.B., Strand, J.A., 1996. Rhizome architecture in *Phragmites australis* in relation to water depth: implications for within-plant oxygen transport distances. Folia Geobot. Phytotax. 31, 91–97.

Weisner, S.E.B., 1996. Effects of an organic sediment on performance of young *Phragmites australis* clones at different water depth treatments. Hydrobiologia 330, 189–194.

Westlake, D.F., 1982. The primary productivity of water plants. In: Symoens, J.J., Hooper, S.S., Compére, P. (Eds.), Studies on Aquatic Vascular Plants. Royal Botanical Society of Belgium, Brussels, pp. 165–180.

Windham, L., Lathrop, R.G., 1999. Effects of *Phragmites australis* (common reed) invasion on aboveground biomass and soil properties in brackish tidal marsh of the Mullica River. New Jersey. Estuaries 22, 927–935.

Wrubleski, D.A., Murkin, H.R., Van der Valk, A.G., Nelson, J.W., 1997. Decomposition of emergent macrophyte roots and rhizomes in a northern prairie marsh. Aquat. Bot. 58, 121–134.

Zhao, K.F., Feng, L.T., Zhang, S.Q., 1999. Study on the salinity-adaptation physiology in different ecotypes of *Phragmites australis* in the Yellow River Delta of China: Osmotica and their contribution to the osmotic adjustment. Est. Coast. Shelf Sci. 49 (Suppl. A), 37–42